DEFLECTION OF A CIRCULAR LIQUID JET ON A FLAT PLATE PERPENDICULAR TO THE FLOW DIRECTION

W. Schach

NATIONAL AERONAUTICS AND SPACE ADMINISTRATION
WASHINGTON, D. C.   MAY 1988

NASA National Aeronautics and Space Administration	Report Documentation Page	

1. Report No. TT-20279	2. Government Accession No.	3. Recipient's Catalog No.

4. Title and Subtitle DEFLECTION OF A CIRCULAR LIQUID JET ON A FLAT PLATE PERPENDICULAR TO THE FLOW DIRECTION		5. Report Date MAY 1988
		6. Performing Organization Code

7. Author(s) W. Schach	8. Performing Organization Report No.
	10. Work Unit No.

9. Performing Organization Name and Address National Aeronautics and Space Administration Washington, DC 20546	11. Contract or Grant No. NASW-4307
	13. Type of Report and Period Covered translation

12. Sponsoring Agency Name and Address NATIONAL AERONAUTICS AND SPACE ADMINISTRATION WASHINGTON, DC 20546	
	14. Sponsoring Agency Code

16. Abstract

The deflection of a flat water jet on a flat plate perpendicular and oblique to the flow direction can be determined with the Prandtl hodograph method. The outer jet shape of the circular water jet for perpendicular impact on a flat plate was measured in tests by Reich and was represented by an empirical equation. The problem can also be discussed mathematically, if the flow to be axisymmetric potential flow is to be considered. For this purpose, the same method which Trefftz established for calculating the contraction of a circular liquid jet can be used.

17. Key Words (Suggested by Author(s))	18. Distribution Statement unclassified-unlimited

19. Security Classif. (of this report) unclassified	20. Security Classif. (of this page) unclassified	21. No. of pages 16	22. Price

NASA FORM 1626 OCT 86

DEFLECTION OF A CIRCULAR LIQUID JET ON A FLAT PLATE PERPENDICULAR TO THE FLOW DIRECTION

W. Schach (in Ravensburg)

1. Introduction

The deflection of a flat water jet on a flat plate perpendicular and oblique to the flow direction can be determined with the Prandtl hodograph method [1]. The outer jet shape of the circular water jet for perpendicular impact on a flat plate was measured in tests by Reich [2] and was represented by an empirical equation. The problem can also be discussed mathematically, if we consider the flow to be axisymmetric potential flow. For this purpose we will use the same method which Trefftz [3] established for calculating the contraction of a circular liquid jet.

2. The Trefftz method

In the following paper we use the same notation as in the Trefftz paper [3] in order to obtain agreement for deriving the equations. The differential equation for the potential ϕ of a rotationally symmetric potential flow is

$$\frac{\partial^2 \varphi}{\partial x^2} + \frac{\partial^2 \varphi}{\partial y^2} + \frac{1}{x}\frac{\partial \varphi}{\partial x} = 0, \tag{1}$$

when the y-axis is the symmetry axis and x is the distance from this axis. If the velocity components in the x and y directions are given by

$$u = \frac{\partial \varphi}{\partial x}, \qquad v = \frac{\partial \varphi}{\partial y},$$

then the Stokes stream function ψ is related to the potential function ϕ by the relationship

$$\frac{\partial \psi}{\partial x} = -x\frac{\partial \varphi}{\partial y}, \qquad \frac{\partial \psi}{\partial y} = x\frac{\partial \varphi}{\partial x} \tag{2}$$

Instead of the two equations (2) we can establish a single equation

$$\frac{\partial \psi}{\partial l} = x\frac{\partial \varphi}{\partial n} \tag{3}$$

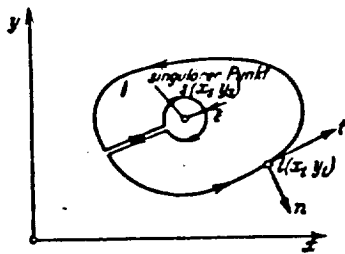*Numbers in margin indicate pagination of foreign text.

Figure 1. Represent-
ation of the integra-
tion path.
1--singular point

for an arbitrary integration path, if the
integration direction t and the normal
direction n are established in such a way
that the t direction corresponds to the y-
axis and the n direction corresponds to the
x-axis of the Cartesian coordinate system
(Figure 1). From (3) we obtain the value
of the stream function as

$$\psi(t) = \int x(t) \frac{\partial \varphi}{\partial n}(t) \, dt. \tag{4}$$

In the following calculations, using the notation of Trefftz
(Figure 1)
s is the singular point where the potential is to be determined
(its coordinates are x_s, y_s),
t is the changing point along the edge of the liquid region, that
is, the integration variable (its coordinates are x_t, y_t).

In order to determine the potential ϕ at a point $s(x_s, y_s)$ of
the liquid region, we will superimpose a source ring flow on to
the desired flow, which has a singularity at point s. The poten-
tial V(st) of this source ring flow satisfies the differential
equation (1). In addition, we postulate that V and its normal
derivative $\partial V / \partial n$ are continuous along the edge of the region. In
addition to the potential function V(st), we can also introduce
a stream function S(st), which is given by the following equation
similar to (4)

$$S(st) = \int x(t) \frac{\partial V(st)}{\partial n(t)} \, dt \tag{5}$$

According to the Green theorem, we have the following equation
which relates the potentials $\phi(st)$ and V(st)

$$\operatorname{div}(V \, x \operatorname{grad} \varphi) - \operatorname{div}(\varphi \, x \operatorname{grad} V) = V \operatorname{div}(x \operatorname{grad} \varphi) - \varphi \operatorname{div}(x \operatorname{grad} V). \tag{6}$$

If we apply the Gauss integration theorem to this equation, then
we obtain

$$\oint \left(V \, x \frac{\partial \varphi}{\partial n} - \varphi \, x \frac{\partial V}{\partial n} \right) dt = 0, \tag{7}$$

where the edge integral is taken over the closed edge of the liquid
region with exclusion of a singular point s (Figure 1).

2

Figure 2. Streamline of a sink ring flow.

Figure 3. Notation according to Trefftz.

If we carry out the limit transition by running the diameter ε of a circle   to 0, then we obtain the following integral equations:
For a point inside the liquid region

$$\varphi(s) = \frac{1}{2\pi} \oint \varphi(t)\, dS(st) - \frac{1}{2\pi} \oint V(st)\, d\psi(t), \qquad (8)$$

For an arbitrary edge point

$$\varphi(s) = \frac{1}{\pi} \oint \varphi(t)\, dS(st) - \frac{1}{\pi} \oint V(st)\, d\psi(t), \qquad (9)$$

For a corner point whose angle = α to the outside

$$\varphi(s) = \frac{1}{2\pi - \alpha} \oint \varphi(t)\, dS(st) - \frac{1}{2\pi - \alpha} \oint V(st)\, d\psi(t). \qquad (9a)$$

The streamline image of the source ring flow is shown in Figure 2. The potential V(st) is determined as

$$V(st) = \frac{2E(\xi)}{\varrho(st)},$$

where we have

$$E(\xi) = \int_0^{\pi/2} \frac{d\sigma}{\sqrt{1 - \xi^2 \sin^2 \sigma}}$$

is the complete elliptical integral of the first kind in the Legendre normal form where

$$\xi = \frac{x_s x_t}{\varrho^2(st)} \qquad \underline{/53}$$

and

$$\varrho(st) = \tfrac{1}{2}(r_1 + r_2)$$

According to Figure 3 we have

$$r_1 = \sqrt{(x_s - x_t)^2 + (y_s - y_t)^2}$$

3

the distance between points t and s,

$$r_2 = \sqrt{(x_s + x_t)^2 + (y_s - y_t)^2}$$

the distance of the point t from s', where s' is the new image
of the point s with respect to the y-axis. The total differential
dS(s t) is calculated as

$$dS(st) = \frac{E(\xi)}{\varrho(st)} dy(t) + \frac{\varrho(st)}{x_s} G(\xi) d\vartheta(st), \qquad (10)$$

where $\vartheta(s,t)$ is the angle between r_1 and r_2 at the point t and
we set

$$G(\xi) = \int_0^{\pi/2} \sqrt{1 - \xi^2 \sin^2 \sigma}\, d\sigma - \frac{1 - \xi^2}{2} \int_0^{\pi/2} \frac{d\sigma}{\sqrt{1 - \xi^2 \sin^2 \sigma}}$$

In equation for G(ξ) the first integral is a complete elliptical
integral of the second kind in the Legendre normal form.

3. Application of the Trefftz method to the deflection of the
    circular jet at a flat plate perpendicular to the flow direction

    a) Assumptions and boundary conditions. The origin of the
corded system is placed at the intersection 0 of the jet axis
and the plate. The plate forms the x-axis, so that the jet center
falls in the y-axis. The liquid region (Figure 4) which is
formed by the axes and the free jet boundary, is delimited by the
axis-parallel line DC and BA at the points where the complete jet
velocity prevails for the incoming and outgoing jet over the
entire cross-section. We will select the distance OD = 1.5 d(d)
= jet diameter) according to experiments of Reich[1]. OA = 2 d
according to our own experiments[2].

    For the jet radius r = 1, the corner points of the liquid
region then have the following coordinates

	A	'B	C	D	O
x	4	4	1	0	0
y	0	0,125	3	3	0

In order to draw in the free jet boundary, we already know its
direction at the point C. At C the tangent is parallel to the

---

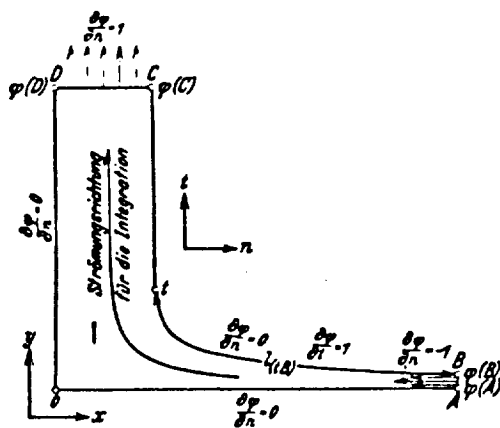1--see footnote 2 of page 51
2--see footnote 1 of page 51

4

Figure 4. Representation of the liquid region. 1--flow direction for integration

y-axis. In its further course, the jet boundary does not differ much from the tangent because (according to Reich) the velocity is not yet highly delayed up to an ordinate value of y = 0.75 d. According to the continuity equation, its free jet boundary of the outflowing jet is a hyperbola xy = const, if the velocity v_1 = const. We can assume that the real jet boundary will approach this hyperbola also before the point B. The varia- /54 tion of the jet boundary in the curvature area first of all has to be established by judgement. For the further calculation, we will set the jet velocity to be v_1 = 1.

In addition to the conditions of axisymmetric potential flow, we have the following boundary conditions (Figure 4) for the edge of the liquid region:

1. Along the y-axis (DO), the x-axis (OA) and the jet boundary (BC) we have $\frac{\partial \varphi}{\partial n} = 0$, because there is no velocity perpendicular to the edge;

2. along DC and AB we have parallel flow, the velocity is v_i = 1, that is we have $\left|\frac{\partial \varphi}{\partial n}\right| = 1$;

3. along the jet edge the velocity is constant, that is $\left|\frac{\partial \varphi}{\partial t}\right| = 1$.

At the points A and B the potential is $\phi(A) = \phi(B)$.

Along the free jet boundary we obtain the potential of the point t according to the boundary condition (3) as follows

$$\varphi(t) = \varphi(B) + l(Bt),\qquad (11)$$

where l(Bt) is the length of the jet edge from B to t. From this we find the potential at the point C to be

$$\varphi(C) = \varphi(B) + l(BC);$$

and at the point D we again have

$$\varphi(D) = \varphi(C).$$

5

In order for $\partial\varphi/\partial t$ to fall in the integration direction along
the jet edge, in order not to always have to use a negative sign,
we consider the flow direction to be reversed.   In other words,
it flows into the region along the line AB and flows away at CD.
This only affects the result in that the potential and its deriva-
tives will have the opposite sign.   Then along the line AB we have

$$\frac{\partial\varphi}{\partial n} = -1,$$

and along the line CD:

$$\frac{\partial\varphi}{\partial n} = +1.$$

b)   <u>The integral equation.</u> According to (9) the potential of
an edge point which is not a corner point is

$$\pi\varphi(s) = \oint\varphi(t)\,dS(st) - \oint V(st)\,d\psi(t).$$

The first integral gives no contribution along the y-axis, because
the y-axis becomes a streamline for the source ring flow (Figure 2)
and therefore dS(st) = 0.   The first edge integral is then simpli-
fied to

$$\oint\varphi(t)\,dS(st) = \int_{\bullet}^{D}\varphi(t)\,dS(st).$$

The second integral

$$\oint V(st)\,d\psi(t) = \oint V(st)\,x(t)\frac{\partial\varphi}{\partial n}(t)\,dt$$

gives no contribution except for AB and CD, because otherwise
$\frac{\partial\varphi}{\partial n} = 0$.   Then we obtain the following when we substitute the
appropriate values for x(t) and dt,

$$\oint V(st)\,d\psi(t) = -x_A\int_{A}^{B}V(st)\,dy(t) + \int_{D}^{C}x(t)\,V(st)\,dx(t).$$

The integral equation therefore is

$$\pi\varphi(s) = \int_{0}^{D}\varphi(t)\,dS(st) + x_A\int_{A}^{B}V(st)\,dy(t) - \int_{D}^{C}x(t)\,V(st)\,dx(t). \qquad (12)$$

The further course of the calculation is as follows: For the   /55
first integration we assume that the singular point s is along
the x-axis.   In this case the x-axis becomes streamline of the
source ring flow and we have

$$\int_{0}^{A}\varphi(t)\,dS(st) = 0,$$

and therefore the potential $\phi(t)$ drops out, which is first unknown
along the x-axis.   From A to D according to (11) we can express
the potential

6

$$\varphi_1(t) = \varphi(B) + l(Bt)$$

and then evaluate all of the integrals. The result is

$$\varphi_1(s) = \varphi(B) + C_1,$$

where C_1 is a numerical value. If we know the variation of the potential along the x-axis for the assumed jet edge with these first integrations, then we will set this singular point along the jet edge. For the potential $\phi(t)$ we set the value $\phi_1(s)$ calculated along the x-axis. On the jet edge and along the following lines we use $\phi_1(t)$ just like for the first integration. The evaluation of the integrals then gives

$$\varphi_2(s) = \varphi(B) + C_2,$$

where C_2 is again a numerical value. The condition that the assumed jet edge is the correct one is the following for the singular point s = t

$$\varphi_2(s) = \varphi_1(t).$$

If this condition is not satisfied, the jet edge has to be selected anew and the same calculation has to be repeated.

c) <u>The evaluation of the integral equation</u>. If the singular point lies along the x-axis (Figure 5), then according to the above the first integral of the equation (12) signifies as follows

$$\int_0^D \varphi(t)\, dS(st) = \varphi(B) \int_A^D dS(st) + \int_B^C l(t)\, dS(st) + l(BC) \int_C^D \varphi(t)\, dS(st).$$
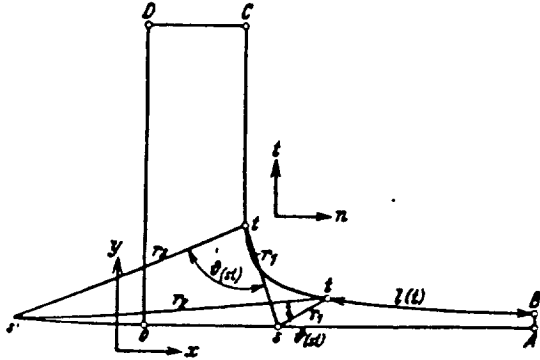

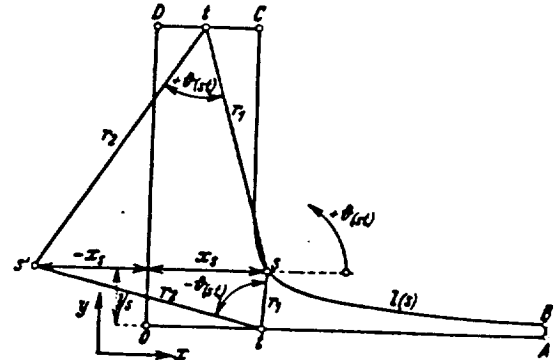Figure 5. The singular point lies on the x-axis

Figure 6. The singular point lies on the jet edge

7

For abbreviation we have introduced l(t) = l(Bt). According to Figure 2 the value of the stream function at the point A is S(SA) = (sA) = π and at the point D it is S(sD) = 2π, so that we have $\int_A^D d\,S(s\,l) = \pi$. The equation for the potential then is

$$\pi \psi_1(s) = \pi \varphi(B) + \int_B^C l(l)\,dS(sl) + l(BC)\int_C^D d\,S(sl) + x_A\int_A^B V(sl)\,dy(l) - \int_D^C x(l)\,V(sl)\,dx(l). \quad (13)$$

After evaluation of the single integrals we obtain the following result using the notation given in Chapter 2:

/56

$$\left.\begin{aligned}
\int_B^C l(l)\,dS(sl) &= \int_B^C l(l)\,\frac{E(\xi)}{\varrho(sl)}\,dy(l) + \frac{1}{x_s}\int l(l)\,G(\xi)\,\varrho(sl)\,d\vartheta(sl), \\
\int_C^D dS(sl) &= 4(y_i - y_i)\int_C^D \frac{x(l)\,G(\xi)}{(1-\xi^2)\cdot\varrho(sl)\,r_1 r_2}\,dx(l), \\
\int_A^B V(sl)\,dy(l) &= -2\int_A^B \frac{E(\xi)}{\varrho(sl)}\,dy(l), \\
\int_D^C x(l)\,V(sl)\,dx(l) &= -2\int_D^C \frac{E(\xi)}{\varrho(sl)}\,x(l)\,dx(l).
\end{aligned}\right\} \quad (13a)$$

With this first integration the potential ϕ_1(t) along the x-axis is represented as a sum of ϕ(B) and a numerical value which will be called l_k(t) so that

$$\varphi_1(l) = \varphi(B) + l_1(l)$$

and we now place the singular point s along jet boundary (Figure 6), then we obtain the potential

$$\pi \varphi_2(s) = \int_0^D \varphi_1(l)\,dS(sl) + x_A\int_A^B V(sl)\,dy(l) - \int_D^C V(sl)\,x(l)\,dx(l).$$

For x_t = x_s the integrand of the first integral becomes infinite. Therefore, we convert the integral equation into

$$\pi \varphi_2(s) = \int_0^D [\varphi_1(l) - \varphi_1(s)]\,dS(sl) + x_A\int_A^B V(sl)\,dy(l) - \int_D^C V(sl)\,x(l)\,dx(l) + \int_0^D \varphi_1(s)\,dS(sl),$$

where

$$\varphi_1(s) = \varphi(B) + l(Bs)$$

The value of the stream function at the point 0 is S(s0) = o), according to Figure 2, whereas at the point D it is S(sD) = 2π. From this we obtain the following with consideration of the transition at the point s

$$\int_0^D \varphi_1(s)\,dS(sl) = \pi\varphi_1(s),$$

8

TABLE 1.

	Kurve 1			2 Kurve 2	
x_s	y_s	$\|\varphi_2(s) - \varphi_1(s)\|$	x_s	y_s	$\|\varphi_2(s) - \varphi_1(s)\|$
1,75	0,307	+ 0,021	1,75	0,306	− 0,008
1,315	0,50	+ 0,039	1,228	0,50	+ 0,012
1,047	1,0	+ 0,034	1,027	1,0	+ 0,008
1,0	3,0	+ 0,018	1,0	3,0	− 0,003

1--curve 1; 2--curve 2
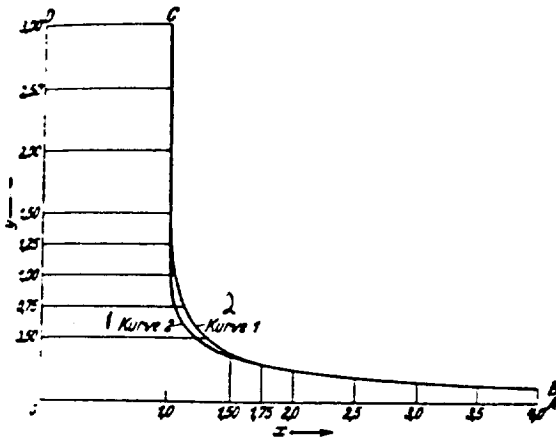
Figure 7. Determination
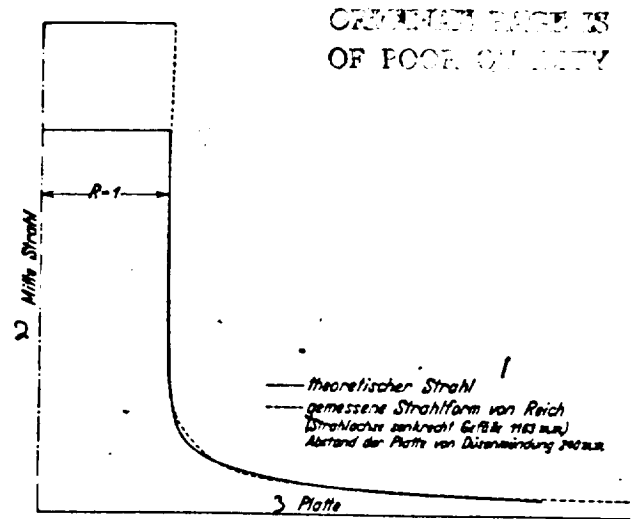of investigated jet shapes.
1--curve 2; 2--curve 1

Figure 8. Comparison of
theoretical jet shape and a
shape measured by Reich.
1--theoretical jet, measured jet
shape of Reich, (jet axis perpen-
dicular to 1163 (illegible)),
distance between plate and
nozzle mouth 240 mm;
2--center of jet; 3--plate

and we can write the following for the integral equation

$$\pi \left[\varphi_2(s) - \varphi_1(s)\right] = \int_0^D \left[\varphi_2(t) - \varphi_1(s)\right] dS(st) + x_A \int_A^B V(st) \, dy(t) - \int_D^C V(st) \, x(t) \, dx(t).$$

If we now substitute values for $\phi_1(t)$ and $\phi_1(s)$ then we obtain

$$\pi \left[\varphi_2(s) - \varphi_1(s)\right] = \int_0^A \left[l_1(t) - l(s)\right] dS(st) - l(s) \int_A^B dS(st) + \int_B^C \left[l(t) - l(s)\right] dS(st) + $$
$$+ \left[l(BC) - l(s)\right] \int_C^D dS(st) + x_A \int_A^B V(st) \, dy(t) - \int_D^C V(st) \, x(t) \, dx(t). \quad (14)$$

The individual integrals may be evaluated similar to (13a). A
similar equation system can be established for the case where the
singular point lies along the y-axis. For the numerical evaluation,
we assume two jet shapes shown in Figure 7. In Table 1 we

9

collect the differences $\phi_2(s) - \phi_1(s)$ for all investigated points.
We can see from Table 1 that for the first curve all of the diff-
erences are positive. For the second curve, there is a difference
of ±0.01. If we assume that these are integration errors, then
the second curve represents the free jet boundary with a good
accuracy. Reich measured the free jet boundary of a jet which
falls down perpendicularly. There is good agreement between the
measured curve and the theoretical curve (Figure 8).

   d)   Velocity and pressure distribution along the plate. The
velocity variation along the plate $u = \frac{\partial \varphi}{\partial x}$ is determined by differ-
entiation of the function $\phi(x)$ with respect to x (Figure 9). We
then obtain the following from the velocity curve according to
the Bernoulli equation

$$p_0 = \frac{\gamma}{2g} v_1^2 \left(1 - \frac{u^2}{v_1^2}\right)$$

as well as the pressure variation along the plate. The theoretical
jet pressure perpendicular to the plate becomes the following for
the assumed boundaries of the liquid region.

$$P_0 = 2\pi \int_0^a x\, p_0\, dx.$$

By graphical evaluation of the integral, we obtain $P_0 = 52.63$ kg.
According to the momentum theorem, for r = 1 and $v_1 = 1$ the
theoretical jet pressure is $P_0 = 50.97$ kg. The deviation is
therefore 3.3%. In order to compare the theoretical pressure
variation with the actual pressure curve, Figure 9 shows the mea-
sured pressure for a nozzle without a needle, recalculated for
the jet radius r = 1 and the jet velocity $v_1 = 1$[1]. In the same
way as for the x-axis, along the y-axis we can find the velocity
variation along the jet axis by differentiation of the function
$\phi(y)$ with respect to y (Figure 10).

   e)   Determination of streamlines and potential lines. In
order to determine the streamlines we use the law for the velocity
distribution of a flow without work, which has the following form

----

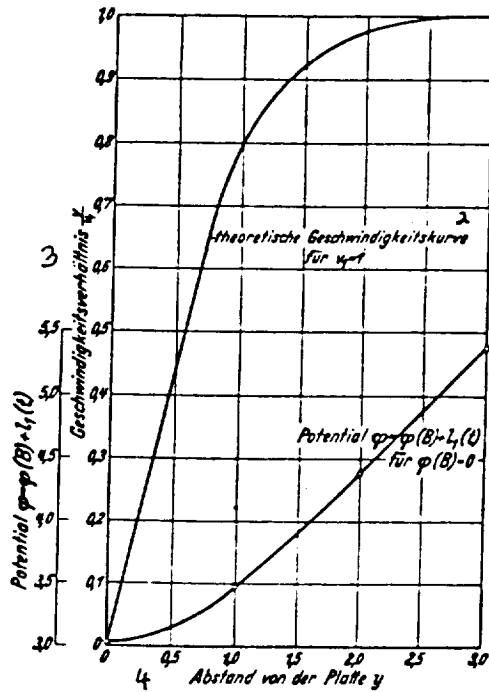[1] W. Schach, see earlier paper in this article.

10

Figure 9. Potential, velocity and pressure distribution along a plate.
1--potential; 2--theoretical velocity curve; 3--velocity ratio; 4--distance from plate y
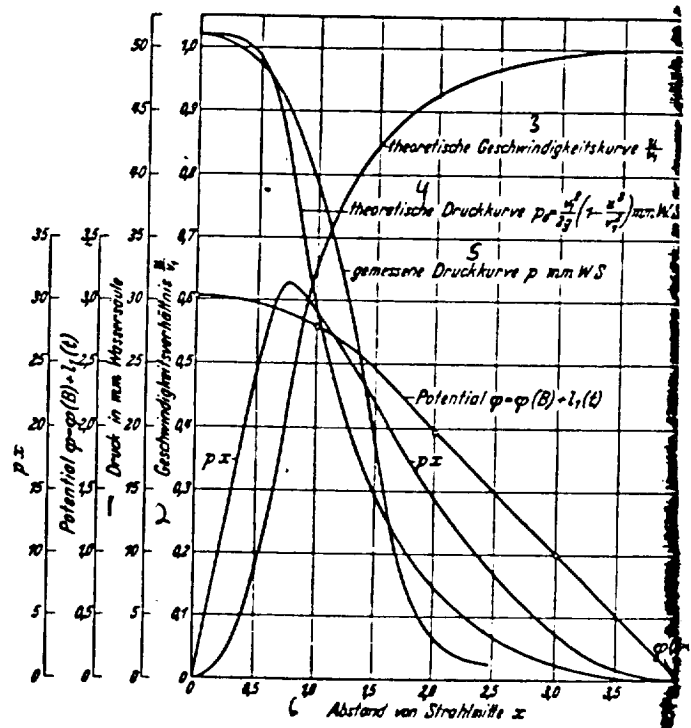
Figure 10. Potential and velocity distribution along the jet axis (y-axis).
1--pressure in mm water column; 2--velocity ratio; 3--theoretical velocity curve; 4--theoretical pressure curve; 5--measured pressure curve p millimeter water column; 6--distance from jet center

along a potential line of the meridional plane vs = const, where s is the distance of two following potential lines. If we consider streamlines which separate layers of equal amounts of water, then we have

$$\Delta Q = 2 r \pi \Delta n,$$

if Δn is the distance between streamlines along the potential line /58 and r is the distance of the center of Δn referred to the y-axis. From this we obtain

$$\frac{s}{\Delta n} = r \cdot const$$

The streamlines form rectangles with the potential lines, and the side ratios are proportional to their distance from the axis of rotation.

11

In the liquid region, two streamlines are known. First of all, the jet boundary, then the y-axis and after this the x-axis. Four partial channels with equal swallowing capacity are assumed. The one between $\psi = 0$ and $\psi = \frac{1}{4}$ is divided in half and the inner half is again subdivided into two equal channels. The distance of the partial channels along the lines AB and CD and is found from the continuity equation (Figure 11). Two following equipotential lines intersect equal length distances along the free jet boundary. The points at equal potential along the x- and y-axis are taken from diagrams in Figures 9 and 10. In order to subdivide the liquid region into rectangles (Figure 11), it is found to be suitable to draw these simultaneously from CD and AB. Then we obtain a good check because even for very small errors in the variation of the streamlines, the two branches will deviate greatly from one another along the potential line $\phi = 0$.

4. <u>Summary</u> Using the Trefftz method, we can transfer the differential equation of the potential

$$\frac{\partial^2 \varphi}{\partial x^2} + \frac{\partial^2 \varphi}{\partial y^2} + \frac{1}{x}\frac{\partial \varphi}{\partial x} = 0$$

into an integral equation

$$\pi \varphi(s) = \int \varphi(t)\, dS(st) - \int V(st)\, d\varphi(t)$$

for an axisymmetric potential flow, by superposition with a source /59 ring flow. This equation applies for a usual edge point. The integrals extend over the edge of the entire region with the exception of the singular point s. When applying this integral equation to the deflection of a circular liquid jet on a flat plate perpendicular to the floor direction, the difficulty in solving the problem is the fact that the jet edge along which the integration is to take place is not known. First of all, we must assume and then from the condition $\partial \varphi/\partial t = \text{const}$ we obtain the potential ϕ_1(s) along the jet edge. Using the integral equation we determine the potential ϕ_1(s) along the x-axis for singular points s of the x-axis. For the second integration, we place the singular point s along the jet edge and calculate ϕ_s(s) from the integral equation. The condition that the assumed jet edge is the correct one is $\varphi_2(s) = \varphi_1(s) = 0$. The numerical
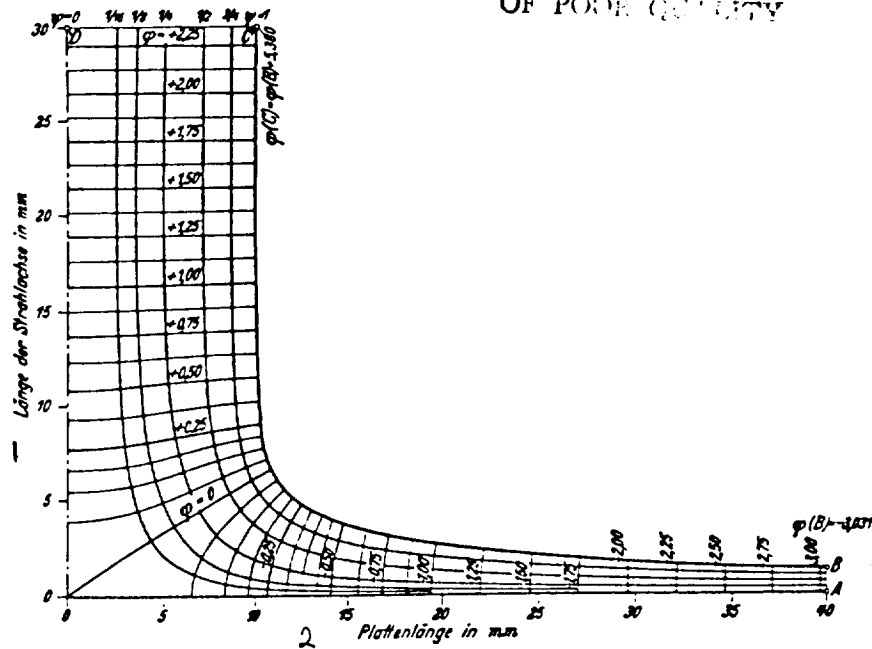
Figure 11. Determination of the streamlines and
potential lines.
1--length of jet axis in mm; 2--plate length in mm

execution resulted in a deviation of ±0.01 for the second assumed
jet edge. If we compare this theoretical jet shape with the
comparison results of Reich, then we obtain very good agreement.

From the variation of the potential over the x-axis, we deter-
mine the velocity and pressure variation along the plate. The
integral

$$P_0 = \int_0^{x_0} 2\pi x p_0 \, dx$$

represents the theoretical jet pressure on a plate. Comparison
with the value P_O determined from the momentum theorem resulted
in a deviation of 3.3%. If the jet boundary is specified, then
the streamlines can be determined with one of the well known
drafting methods, or with electrical experiments.

(Communications from the Institute for Water Machines of
the Technical University Hannover).

(Recd. November 28, 1934)

13

REFERENCES

1. W. Schach. Deflection of a free liquid jet on a flat plate. Dissertation Hannover or Ing-Arch. 5 (1934), p 245.

2. Fr. Reich. Deflection of a free liquid jet on a flat plate perpendicular to the floor direction. Dissertation Hannover 1926 or VDI Research Journal 290.

3. E. Trefftz. The contraction of circular liquid jets. Dissertation Strasburg 1914. Also Z. Math. Phys. 64 (1916) p 34.